BRAIN CONNECTIVITY
Volume 11, Number 7, 2021

DOI: 10.1089/brain.2020.0901

Effect of Stroke on Contralateral Functional Connectivity

Grigori Yourganov,[1] Brielle C. Stark,[2,3,i] Julius Fridriksson,[4] Leonardo Bonilha,[5] and Christopher Rorden[6]

Abstract

Introduction: Stroke can induce large-scale functional reorganization of the brain; however, the spatial patterns of this reorganization remain largely unknown.
Methods: Using a large ($N = 116$) sample of participants who were in the chronic stages of stroke, we present a systematic study of the association between brain damage and functional connectivity (FC) within the intact hemisphere. We computed correlations between regional cortical damage and contralateral FC.
Results: We identified left-hemisphere regions that had the most pronounced effect on the right-hemisphere FC, and, conversely, right-hemisphere connections where the effect of damage was particularly strong. Notably, the vast majority of significant correlations were positive: damage was associated with an increase in regional contralateral connectivity.
Discussion: These findings lend evidence of the reorganization of contralateral cortical networks as a response to brain damage, which is more pronounced in a set of well-connected regions where connectivity increases with the amount of damage.

Keywords: aphasia; connectivity; fMRI; plasticity; stroke

Impact Statement

The relatively large sample size combined with our best-of-breed analysis methods provides us with sufficient statistical power and spatial sensitivity to identify a set of brain regions where damage has the strongest impact on contralateral networks, and a set of contralateral functional connections that increase in strength in response to brain damage. Our results demonstrate that the brain's ability to reorganize itself after extensive damage is not distributed equally in space, but is more likely to occur in specific core regions. We believe that the associations between brain damage and increased connectivity in the ''intact'' hemisphere provide novel, and important, insight into the plasticity of the adult brain.

Introduction

Stroke has a profound effect on the brain, which extends well beyond lesioned areas (Carrera and Tononi, 2014). The axonal connections between the lesioned and spared brain regions undergo the process of Wallerian degeneration (Thomalla et al., 2005), leading to widespread disruptions of the anatomical connectome (Bonilha et al., 2014). On the contrary, spontaneous recovery from stroke is at least partially supported by sprouting of new axonal connections, as demonstrated in animal models (Carmichael et al., 2001; Lindau et al., 2013; Overman et al., 2012; Wahl et al., 2014). These structural changes lead to a complex pattern of abnormal brain activity in spared brain regions, which varies with time, lesion volume and location, and the progress of recovery (Anglade et al., 2014; Grefkes and Fink, 2014; Hartwigsen and Saur, 2017). In patients with moderate or severe poststroke functional impairment, abnormal activity in terms of electrophysiological, metabolic, and hemodynamic response has been observed in the contralateral as well as the ipsilesional hemisphere [see review by Cocquyt et al. (2017)].

Some of the stroke-induced increase of contralateral activity (as measured using functional magnetic resonance imaging [fMRI]) likely reflects functional reorganization of cortical

[1]Advanced Computing and Data Science, Cyberinfrastructure and Technology Integration, Clemson University, Clemson, South Carolina, USA.
[2]Department of Speech, Language and Hearing Sciences, Indiana University, Bloomington, Indiana, USA.
[3]Program in Neuroscience, Indiana University, Bloomington, Indiana, USA.
Departments of [4]Communication Science and Disorders and [6]Psychology, University of South Carolina, Columbia, South Carolina, USA.
[5]Department of Neurology, Medical University of South Carolina, Charleston, South Carolina, USA.
[i]ORCID ID (https://orcid.org/0000-0002-7001-8324).

networks, which can supplant recovery in some participants. However, this signal may also be elicited by disinhibition, reflecting a maladaptive response in other participants. Therefore, the role of the contralateral hemisphere in poststroke recovery remains controversial (Cocquyt et al., 2017). For example, Anglade and associates (2014) propose a model where the subacute phase of recovery (3 weeks to 6 months after the stroke) is associated with an increase of neuronal activity in the contralateral hemisphere; in the chronic stage (>6 months poststroke), this activity shifts to the ipsilesional hemisphere in cases of successful recovery, but persists in the contralateral hemisphere in cases of weak recovery (Saur et al., 2006). The observation of a shift in activity from contra- to ipsilesional cortex opens the possibility of facilitating poststroke recovery by modifying the contralateral activity with noninvasive brain stimulation, such as transcranial magnetic stimulation (TMS) (Di Pino et al., 2014) and transcranial direct current stimulation (tDCS) (Kang et al., 2018).

The poststroke change in patterns of brain activity is accompanied by a change in functional connectivity (FC), that is, in synchronization of blood-oxygen-level-dependent imaging (BOLD) signal within cortical networks. The most robust result is the association between behavioral impairment and a decrease in interhemispheric FC, observed, in particular, within homotopic regions [for various types of behavioral impairment, this was reported by Carter and colleagues (2010); Baldassare and colleagues (2014); Xu and colleagues (2014); New and colleagues (2015); Bannister and colleagues (2016); Siegel and colleagues (2016, 2018); Tang and colleagues (2016); Adhikari and colleagues (2017); Sandberg (2017); Yang and colleagues (2017)]. This poststroke reduction in homotopic FC might have two possible causes. The first cause is the direct effect of the lesion: if the BOLD signal of the infarcted brain regions is essentially noise, the correlation with the BOLD signal measured at intact contralateral parts of the network must be small. The second cause follows from diaschisis, where the FC between intact regions of a network is reduced as an effect of damage to a remote cortical region [this could be detected by excluding lesioned areas from the FC analysis; see, e.g., Carter and associates (2010); Baldassare and associates (2014); Tang and associates (2016); and Siegel and associates (2016)]. A question remains, however: What is the impact of stroke on the FC *within* the contralateral (intact) hemisphere?

Studies by Nair and associates (2015) and Siegel and associates (2016) report no significant difference in contralateral FC between chronic stroke patients and age-matched healthy controls. On the contrary, Zhang and colleagues (2017) report an increase in FC between contralateral middle frontal and superior parietal regions in chronic stroke. Gili and colleagues (2017), using the graph-theoretical approach to study therapy-induced changes in the contralateral network of aphasia patients, report a post-therapy increase in eigenvalue centrality of Brodmann areas 6 (premotor cortex/supplementary motor area) and 21 (middle temporal gyrus) accompanied by significant behavioral improvement.

Here, we systematically address the question of the effect of stroke on FC *within* the contralateral hemisphere. For this purpose, we utilize structural and resting-state functional neuroimaging data acquired in a large group of individuals with chronic left-hemisphere stroke ($N = 116$). Strokes most typically included portions of the left middle cerebral artery territory, but the size and location of the lesion varied across participants. Rather than limiting our analysis to predefined resting-state networks, we look at all functional connections between the regions of the contralateral hemisphere. Specifically, we use a parcellation of gray matter (Joliot et al., 2015) that provides us with a large number of parcels (384 for the whole brain) of roughly similar size. This approach gives us enough statistical power and spatial sensitivity to answer two important questions: (1) Which functional connections in the contralateral hemisphere are most affected by the total amount of stroke-related brain damage and (2) what are the ipsilesional brain regions where damage has the strongest impact on contralateral FC?

Materials and Methods

Participants

Participants were recruited from the local community. The research was approved by the Institutional Review Board at the University of South Carolina and at the Medical University of South Carolina. Written consent was obtained from all participants. Only individuals with a single ischemic or hemorrhagic stroke involving the left-hemisphere were included. Participants with lacunar infarcts or with damage that only involved the brainstem or cerebellum were excluded. The participants were scanned between June 2007 and April 2018, and 116 individuals were included in the data analyses. The mean ± standard deviation (SD) age was 59.1 ± 10.6 years (range, 29–81 years), and 23 were women. All participants were at least 6 months poststroke at the time of neuroimaging acquisition, and the mean ± SD time since stroke onset was 38.1 ± 50.5 months (range, 6–276 months). The participants were recruited as part of a larger study of aphasic impairment associated with left-hemisphere stroke (see Funding Information section for grant numbers); however, 21 participants out of 116 exceeded the cutoff for clinical aphasia (their aphasia quotient as measured by Western Aphasia Battery (Kertesz, 2007) was greater than the clinical cutoff threshold of 93.8). See Table 1 for a breakdown of demographics.

Data acquisition

Images were acquired on a Siemens Trio 3T scanner (equipped with a 12-element head coil) and a Siemens Prisma 3T scanner (equipped with a 20-element head/neck coil) located at the University of South Carolina and at the Medical University of South Carolina. Three images relevant for this work were acquired for each participant:

1. T1-weighted image utilizing an MP-RAGE sequence with 1 mm isotropic voxels, a 256 × 256 matrix size, 9° flip angle, and 192 slices (TR = 2250 msec, TI = 925 msec, TE = 4.15) with parallel imaging (GeneRalized Autocalibrating Partial Parallel Acquisition [GRAPPA] = 2, 80 reference lines). The sequence required ∼7 min to acquire.
2. T2-weighted image using a sampling perfection with application optimized contrasts using a different flip angle evolution (3D-SPACE) sequence. This 3D TSE scan uses a TR = 2800 msec, a TE of 402 msec, variable flip angle, 256 × 256 matrix scan with 176 slices (1 mm thick), using parallel imaging (GRAPPA = 2, 80 reference lines). This used the same slice center and angulation as the T1 scan.

Table 1. Demographics for Included Participants, All of Whom Were at Least 6 months Poststroke to the Left-Hemisphere

Demographics	*M (SD)*
Age at assessment in years	59.33 (10.47)
Aphasia severity[a] Max score allowed = 100 (no aphasia)	63.46 (28.40)
Months poststroke at assessment	38.31 (50.69)
Aphasia subtype	24 Anomic 42 Broca's 12 Conduction 9 Global 1 Isolation 1 Transcortical sensory 0 Transcortical motor 6 Wernicke's 21 Not aphasic by WAB ("Latent aphasia")

A wide range of aphasia subtypes and severities are demonstrated.
[a]As measured by the Western Aphasia Battery Aphasia Quotient.
SD, standard deviation.

3. Resting-state fMRI: one functional run was acquired, and the participants were instructed to stay still during the acquisition. For 49 participants (scanned with the 12-channel coil on a Trio scanner), we acquired an EPI sequence with 196 volumes, a 208 × 208 mm field of view, a 64 × 64 matrix size, and a 75° flip angle, 34 axial slices (3 mm thick with 20% gap yielding 3.6 mm between slice centers), TR = 1850 msec, TE = 30 msec, GRAPPA = 2, 32 reference lines, sequential descending acquisition. For the remaining 67 participants (scanned with a 20-channel coil after the scanner was upgraded to the Prisma platform), we used a multiband sequence (x2) with a 216 × 216 mm field of view, a 90 × 90 matrix size, and a 72° flip angle, 50 axial slices (2 mm thick with 20% gap yielding 2.4 mm between slice centers), TR = 1650 msec, TE = 35 msec, GRAPPA = 2, 44 reference lines, interleaved ascending slice order. For 50 participants out of 67, 427 volumes were acquired; for the remaining 17 participants, 370 volumes were acquired.

Preprocessing of structural scans

Lesions were manually drawn on the T2-weighted image by a neurologist. The T2 image was coregistered to the T1 image, and these parameters were used to reslice the lesion into the native T1 space. The resliced lesion maps were smoothed with a 3-mm full-width half-maximum (FWHM) Gaussian kernel to remove jagged edges associated with manual drawing. We then performed enantiomorphic normalization (Nachev et al., 2008) using the SPM12 and MATLAB scripts we developed (Rorden et al., 2012) as follows: first, a mirrored image of the T1 scan (reflected around the midline) was created, and this mirrored image was coregistered to the native T1 image. We then created a chimeric image based on the native T1 scan with the lesioned tissue replaced by tissue from the mirrored scan (using the smoothed lesion map to modulate this blending, feathering the lesion edge). SPM12's unified segmentation-normalization (Ashburner and Friston, 2005) was used to warp this chimeric image to standard space, with the resulting spatial transform applied to the actual T1 scan as well as the lesion map. The normalized lesion map was then binarized by thresholding at 0.5. Lesion size was computed as the number of voxels in the normalized binary lesion map. Figure 1A shows the overlap of lesions for our sample of participants.

To assess regional brain damage, we used the parcellation of gray matter developed by Joliot and colleagues (2015). The T1-weighted image was segmented into probabilistic gray and white matter maps, and the gray matter map was divided into 384 regions according to the atlas. In our sample,

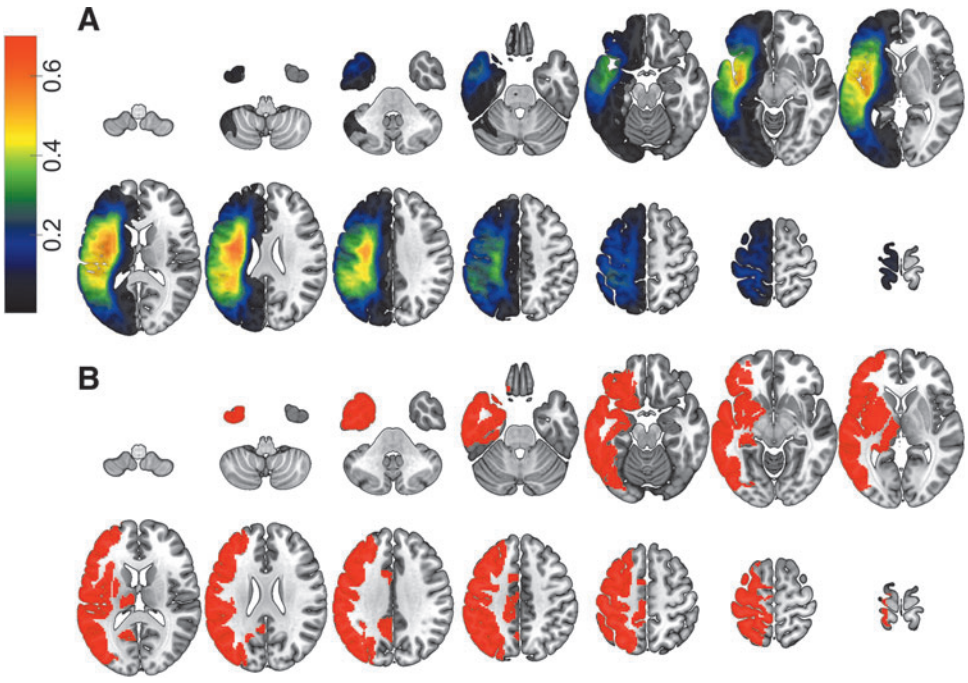

FIG. 1. **(A)** Overlap of lesions in our sample of 116 participants (with the voxel color indicating the proportion of participants having a lesion at that location). **(B)** Gray matter regions that are damaged in at least 20% of our participant sample. Color images are available online.

participants with large lesions had enlarged lateral ventricles (ipsilesional as well as contralateral); since the caudate nucleus is located immediately next to the lateral ventricles, ventricular enlargement created a problem with aligning the caudate across participants. Therefore, we excluded the regions of interest (ROIs) that were located within the caudate. For the remaining 354 ROIs (177/hemisphere), we computed the regional damage as the ratio of the number of lesioned voxels within the ROI to the total number of voxels in the ROI. Figure 1B displays the ROIs that were damaged in at least 20% of our participants.

Preprocessing of fMRI

The resting-state fMRI data were corrected for motion using the SPM12 ''realign and unwarp'' procedure with default settings. After that, we performed brain extraction using the SPM12 script spm_brain_mask with default settings. Slice time correction was also done using SPM12 (for the 67 participants acquired with a multiband sequence, this step was skipped). After that, the mean fMRI volume for each participant was aligned to the corresponding T2-weighted image to compute the spatial transformation between the fMRI data and the lesion mask. The fMRI data were then spatially smoothed with a Gaussian kernel with FWHM = 6 mm. The voxel-wise fMRI time courses were detrended using the following regressors: mean signals from the white matter and from cerebrospinal fluid; time courses of the six motion parameters estimated at the motion correction step; linear, quadratic, and cubic trends. Then, the time courses were bandpass-filtered using the 0.01–0.1 Hz frequency band. After these steps, FC for a pair of ROIs was computed as Pearson's correlation coefficient between their mean fMRI time courses. For this study, we focused on the connectivity within the ROIs in the right (contralateral) hemisphere; given the 177 right-hemisphere gray-matter ROIs, contralateral FC comprised 15,576 functional connections.

To evaluate the participant's motion, we computed mean frame displacement as outlined in Power and colleagues (2012). We used the rigid-body translation and rotation parameters estimated during the motion correction step to compute frame-to-frame displacement as the sum of translational and rotational displacement (for rotational displacement, we used the head radius of 50 mm). Mean frame displacement was estimated as the average of frame-to-frame displacements. Due to the short duration of some of our scanning sequences (6 min), we did not perform motion scrubbing as outlined in Power and colleagues (2012); instead, we identified the contralateral functional connections that were significantly correlated with mean frame displacement, and discarded them from the analysis.

Results

Influence of lesion size on contralateral FC

There was a large variation in lesion size in our participant sample (range: 164–467,458 mm^3; mean: 114,297 mm^3; median: 95,852 mm^3; SD: 99,162 mm^3; interquartile range: 141,766 mm^3). Lesion size was not significantly different across the participants scanned with different fMRI sequences ($p > 0.09$). The size of the lesion had an impact on the FC in the right (contralateral) hemisphere: Pearson's correlation between lesion size and mean value of FC (computed across all pairs of right-hemisphere ROIs) was 0.4444 ($p = 0.0000006$), and between median value of FC was $r = 0.4261$ ($p = 0.0000019$). The scatterplots of lesion size versus mean/median contralateral FC are shown in Supplementary Figure S1.

To identify which contralateral connections were most impacted by lesion volume, we correlated the strength (r-values) of the 15,576 functional connections between right-hemisphere ROIs with lesion size. Supplementary Figure S2 shows the distribution of the resulting correlations. To correct for multiple comparisons, we controlled the false discovery rate (Benjamini and Hochberg, 1995) at $\alpha = 0.05$. One thousand forty out of 15,576 correlations survived this correction. After discounting the 212 functional connections that were correlated with mean frame displacement as well as with lesion volume, we ended up with 828 correlations. The vast majority of them (821 out of 828) were positive correlations, that is, greater lesion size was associated with increased contralateral FC. The strongest 10% of these positive correlations are displayed in Figure 2A. Figure 2B shows the contralateral ROIs involved in the functional connections, which were affected by lesion size. The impact of lesion was most prominently associated with increased strength (r-value) of contralateral functional connections that involve regions around the temporoparietal junction (including supramarginal gyrus and posterior part of superior temporal gyrus), posterior parts of occipital lobe, insula, Rolandic operculum, inferior frontal gyrus, and the orbital part of middle frontal gyrus. Medially, this effect is observed most prominently in the posterior cingulate gyrus, hippocampus, and precuneus.

The effect of lesion volume on contralateral FC was not mediated by gender and scanner type. No right-hemisphere connections showed significant group differences in correlations between lesion volume and connectivity (converted to Z scores via Fisher's r-to-Z transform) when corrected for multiple comparison (gender: $p > 0.8$; scanner type: $p > 0.9$). The participant's age at the time of scanning had no correlation with any contralateral functional connections ($p > 0.3$). To test for the interaction between age, lesion volume, and contralateral FC, we computed the product of age and lesion volume and regressed out both age and lesion volume (Cohen and Cohen, 1983, p. 305); then, we computed the correlation between the residuals and the contralateral functional connections. No correlations were significant ($p > 0.9$). We repeated the analysis to test for the effect of the number of months poststroke; likewise, no significant results were found (correlations between months poststroke and contralateral FC: $p > 0.3$; interaction analysis: $p > 0.9$).

In addition, we investigated the effect of lesion volume on the betweenness centrality of the right-hemisphere ROIs. Betweenness centrality is a graph-theoretical measure computed for the nodes of the network as the proportion of all the shortest paths in the network, which pass through a given node; if this proportion is high, the node is a network hub (Rubinov and Sporns, 2010). After correcting for multiple comparisons, we found no right-hemisphere ROIs where betweenness centrality was significantly correlated with lesion volume ($p > 0.15$ for all contralateral ROIs).

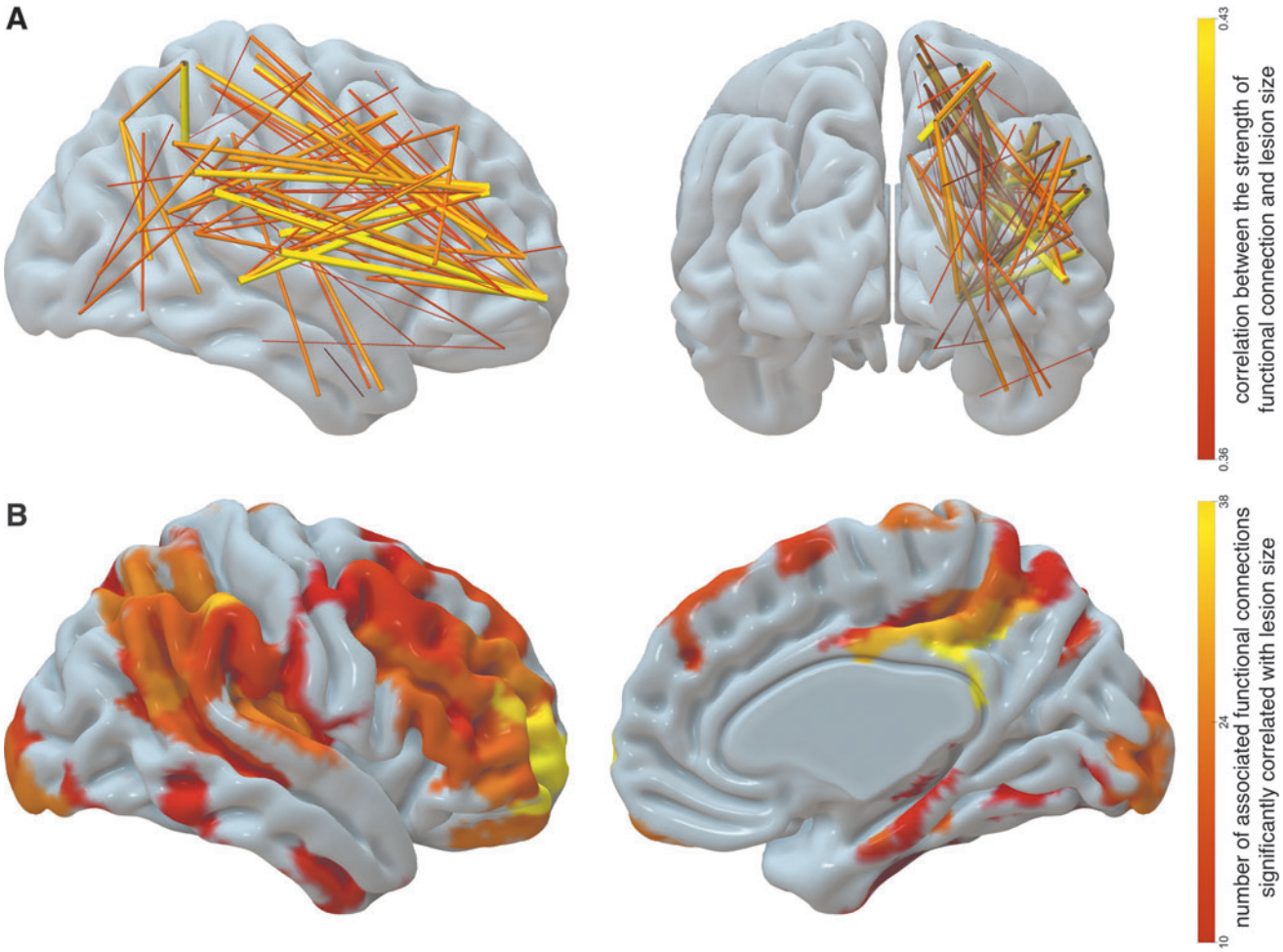

FIG. 2. **(A)** Contralateral functional connections that have the strongest correlation with lesion size (only strongest 10% of 828 such connections are displayed). The width and color indicate the strength of correlation with lesion size. **(B)** Contralateral regions associated with functional connections that are significantly correlated with lesion size. The color of the ROI encodes the number of functional connections stemming from that ROI, which are significantly correlated with lesion size; only ROIs with at least 10 such connections are displayed. ROI, region of interest. Color images are available online.

Influence of regional damage on contralateral FC

The next question pertained to localizing brain regions in the ipsilesional hemisphere, which, when lesioned, have a strong impact on FC in the contralateral hemisphere. For this purpose, we computed a set of correlation coefficients between the amount of regional damage in left-hemisphere ROIs and the FC within the homologue right-hemisphere ROIs. We only considered the left-hemisphere ROIs that had nonzero damage in at least 20% of our participants; this was observed in 105 ROIs, shown in Figure 1B. We computed the correlation between the proportion of damage in each ROI (ratio of the number of lesioned voxels to the ROI size) and contralateral FC values for each pairing of the 177 right-hemisphere ROIs (15,576 functional connections in total). In total, we computed a set of $105 \times 15{,}576 = 1{,}635{,}480$ correlation coefficients and the associated p-values, which were corrected for multiple comparisons by controlling for the false discovery rate using the Benjamini/Hochberg procedure at alpha = 0.05. One hundred fifty-five correlations survived multiple comparisons correction. Then, we discarded the functional connections that were significantly correlated with mean frame displacement (and survived the FDR multiple comparisons correction). This yielded 125 correlations; all of them were positive, that is, damage to a left-hemisphere ROI was associated with *increased* right-hemisphere FC. Table 2 lists the ROIs where damage was correlated with the strength of at least two contralateral functional connections; these ROIs are visualized in Figure 3. The largest number of significant correlations was found for two left-hemisphere ROIs located within the central sulcus (five and seven correlations); four significant correlations were found for an ROI in the supramarginal gyrus; three significant correlations were found for an ROI in the postcentral gyrus; two ROIs within the Rolandic operculum; and one ROI in anterior insula. Figure 4 displays the functional connections in the right (contralateral) hemisphere that were significantly correlated with the damage in each of the seven left-hemisphere ROIs listed above. To see whether the number of significant correlations between contralateral FC and damage to the specific ROI was related to the amount of damage, we correlated it with the across-subject average of proportion of damage to each ROI (Pearson's $r = 0.3646$; $p = 0.00013$).

Table 2. Left-Hemisphere Gray Matter Regions of Interests (According to the AICHA Atlas) Where the Proportion of Damage Correlates with the Strength of at Least Two Contralateral Functional Connections

Left-hemisphere ROI	*No. of significantly correlated contralateral functional connections*
Anterior insula 4	14
Rolandic operculum 1	14
Putamen 3	14
Central sulcus 1	9
Rolandic operculum 2	9
Postcentral sulcus 1	8
Posterior insula 1	8
Anterior insula 3	6
Inferior frontal gyrus, pars triangularis 1	4
Superior temporal gyrus 3	4
Precentral sulcus 4	3
Postcentral sulcus 2	3
Postcentral sulcus 3	3
Supramarginal gyrus 1	3
Anterior insula 5	3
Superior temporal gyrus 2	3
Supramarginal gyrus 3	2
Superior frontal sulcus 2	2
Anterior insula 2	2
Putamen 2	2

ROI, region of interest.

Discussion

Using a large cross-sectional sample of chronic stroke participants, we evaluated the long-lasting impact of stroke on FC within the contralateral hemisphere. In general, larger lesions were associated with higher contralateral FC, and lesion volume was *positively* correlated with the average FC within the contralateral hemisphere. It has been reported previously (Golestani et al., 2013) that the immediate effect of stroke on FC is negative, but in the late acute stage (>7 days post-stroke), FC is not significantly different from age-matched controls, which suggests a process of functional reorganization during the acute stage. We speculate that larger lesions (which also cause lasting functional behavior impairments, as was seen in this sample re: aphasia) cause more prominent functional reorganization, associated with an increase in FC persisting into the chronic stage. The cross-sectional nature of our studies precludes us from drawing strong conclusions about the temporal process of such reorganization; this would be a direction for future longitudinal studies with sufficient statistical power.

The impact of the lesion is most pronounced in functional connections that involve a particular set of brain regions, displayed in Figure 2. These brain regions are involved in many bilateral functional networks, such as somatosensory, motor, memory, interoceptive, salience, and default-mode networks, along with, possibly many others. Therefore, the reported effect (of ipsilateral damage correlating with contralateral FC) is not specific to any particular functional network. Many of these regions (such as dorsal anterior cingulate cortex, precuneus, and posterior occipital lobe) have been described as

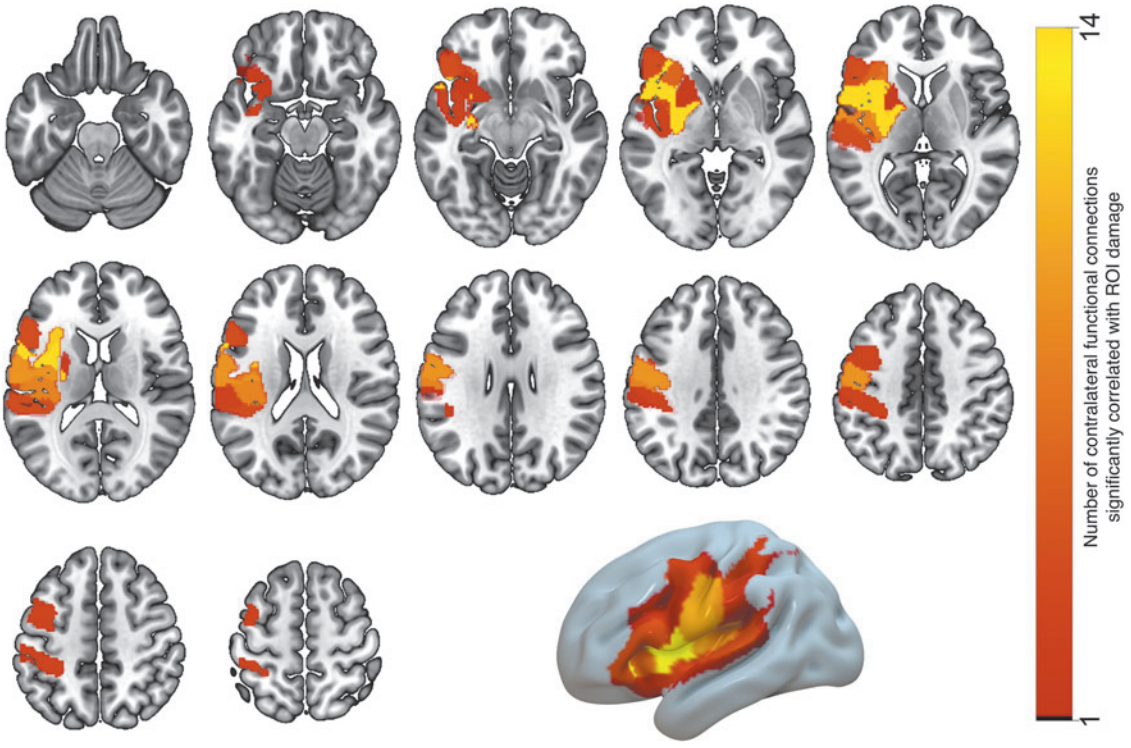

FIG. 3. Gray matter ROIs (listed in Table 1), where the proportion of damage is significantly correlated with the strength of at least two contralateral functional connections. The number of functional connections associated with damage to each ROI is indicated by the ROI color. Color images are available online.

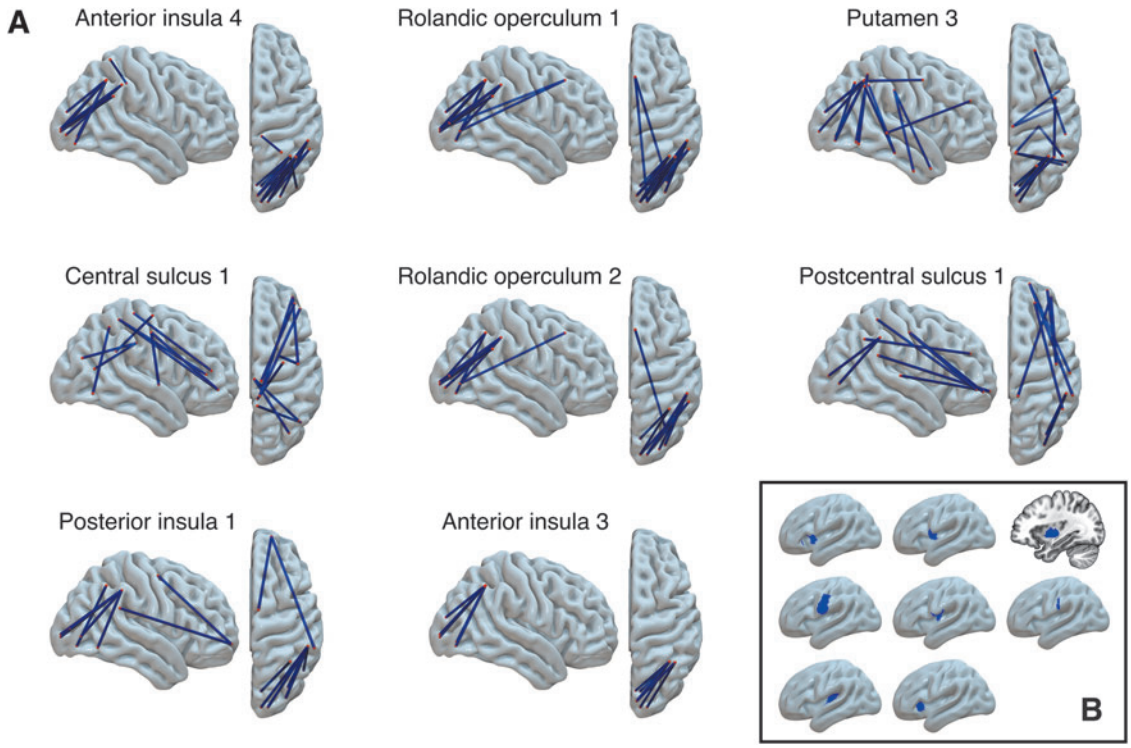

FIG. 4. **(A)** Contralateral functional connections that are positively correlated with damage in eight specific lesioned ROIs (i.e., functional connectivity is greater in people with greater ROI damage). **(B)** Location of these seven ROIs in the left-hemisphere. Color images are available online.

network hubs of the brain (van der Heuvel and Sporns, 2013), which play a particularly important role in communicating and integrating information due to their high degree of connectivity to other regions. Perhaps high correlations with lesion size, observed in functional connections stemming from some of these hub regions, could be explained by their pivotal role within brain networks, such that poststroke reorganization of networks is most prominent in these central nodes of the brain (but it should also be noted that we did not find evidence for effect of lesion size on right-hemisphere regional betweenness centrality). However, the observed effect cannot be fully explained by regional centrality: for example, contralateral sensorimotor regions located around the central sulcus, despite being reported as network hubs (van der Heuven and Sporns, 2013), did not show significant correlation between their FC and lesion size. Another possible explanation, and an exciting direction for future research, could be that the regions in Figure 2 have a higher potential to reorganize after a stroke, either through sprouting of new synapses or through reactivation of previously silent synapses, irrespective of their functional specialization or hub-status. Leveraging network measures, such as mesoscale structure (Betzel et al., 2018) as well as other metrics of communality, such as clustering coefficient (Sporns et al., 2004), in longitudinal designs will be able to evaluate the reorganization potential in these areas. Grefkes and Fink (2014) emphasize the use of such network measures for stroke recovery research.

The location of the lesion plays a role in the reorganization of the contralateral networks. We have demonstrated a set of left-hemisphere areas where regional damage has a particularly high correlation with right-hemisphere FC. These correlations remain significant after we correct for multiple comparisons across more than 1.5 million pairings of left-hemisphere ROIs and right-hemisphere functional connections. Comparing Figures 2 and 3, it is interesting to see a lack of symmetry: the set of right-hemisphere regions where the connectivity is most sensitive to contralateral damage (Fig. 2) and the set of left-hemisphere regions where damage has the most impact on contralateral connectivity (Fig. 3) are not entirely symmetrical (however, symmetry is observed in the supramarginal gyrus, insula, and Rolandic operculum). This is interesting, given that functional connections between the homologues are among the most robust functional connections in the healthy brain (Mišić et al., 2014). However, we show that the impact of regional damage spreads far beyond the functional connections of the homologues; for example, damage to insular/opercular regions was associated with increased connectivity between areas that were far from the contralateral homologues, such as long-range parieto-occipital and parieto-temporal connections (Fig. 4).

Because our study utilized a large sample of participants with a wide range of lesion volume, we were able to identify several contralateral functional connections that were correlated with lesion volume. This method might be more powerful than the comparison of functional connections in stroke patients versus age-matched healthy controls, because FC in healthy individuals varies widely across subjects (Finn et al., 2015) and might not be statistically different from FC in participants with small lesions. This could explain the lack of significant difference in FC reported by Nair and colleagues (2015) and by Siegel and colleagues (2016).

To increase spatial sensitivity of our analysis, we used a brain atlas that parcellated gray matter into a fairly high number of ROIs (177/hemisphere). However, the statistical power of our analysis is influenced by spatial distribution of lesions and, ultimately, by vasculature (Shahid et al., 2017). It is possible that our analysis has missed some brain regions where damage is rare, but nevertheless has a considerable impact on the function of contralateral networks. Moreover, due to the nature of participant recruitment in our study, our data are representative of the population of stroke survivors who have speech/language impairment (which is a common symptom in left middle cerebral artery stroke) and enroll to seek therapy. Therefore, we have insufficient statistical power to identify brain regions supplied by anterior and posterior cerebral arteries. However, due to the large sample size ($N = 116$), our results are not entirely driven by the spatial pattern of damage. For example, temporal regions are damaged in a large portion of our participant sample (Fig. 1), but damage in the majority of temporal regions is not significantly correlated with contralateral FC; on the contrary, damage to the inferior frontal sulcus and intraparietal sulcus is significantly correlated with contralateral FC, despite being lesioned less frequently.

Our study focuses on the relationship between chronic damage and contralateral FC; a natural next step would be to see whether this relationship is relevant for behavioral performance. In particular, since severity and recovery of poststroke aphasia are influenced by left-hemisphere damage and possibly by consequent right-hemisphere reorganization, a logical next step is to evaluate how our results relate to behavioral measures of speech and language. Motor function is also of particular interest, given the observed effect of damage to primary sensorimotor regions on contralateral networks. In addition to large cross-sectional studies, longitudinal studies are needed to investigate the time course of contralateral reorganization and its relevance for behavioral recovery. Another interesting direction would be to see if our results are symmetrical, that is, to investigate the effect of right-hemisphere lesions on FC within the contralateral left-hemisphere. Clinically, the understanding of the contralateral hemisphere's reorganization—and indeed, being able to predict its reorganization pattern given ipsilesional metrics such as overall lesion volume and, more crucially, regional damage in critical ROIs—will allow us to improve prognostication in stroke and leverage neuromodulatory therapies (e.g., tDCS, TMS) and behavioral therapies shown to activate specific contralateral regions, thus improving the recovery potential. These findings are incredibly valuable to prognostication and understanding the mechanisms of recovery in persons living with chronic poststroke aphasia—the population of interest of the present study—because these factors remain poorly understood.

The results that we have shown here—significant changes in FC within the contralateral hemisphere in persons with relatively large chronic stroke lesions—could be further appreciated in future studies. One interesting next step would be to evaluate edge FC (which they call eFC), as per a recent article by Faskowitz and colleagues (2020), describing the relationship between edges (connections) rather than nodes. While tradition FC is calculated between nodes (or regions, as we have done here), eFC is the correlation between two sets of edges/connections. In this framework, brain regions with weak node FC may still exhibit strong eFC, demonstrating that the two areas may be engaged in a similar pattern of communication, even if they are not strongly communicating with each other. Therefore, evaluating eFC has the potential to more comprehensively estimate the changes in contralateral FC in chronic stroke, as a change in the overall pattern of communication may also be present in the contralateral hemisphere. Another future direction would be dynamic FC—that is, quantifying the change in the temporal aspect of contralateral FC in relation to ipsilesional lesion damage (Allen et al., 2014). Recent work has also demonstrated that macroscale brain features can be mapped to low-dimensional manifold representations, or gradients, and identify cortex-wide patterns associated with behavior (as discussed earlier, e.g., speech, language, motor), or to examine similarities in gradients across clinical conditions (e.g., between subtypes of aphasia, which typically associate with distinct left-hemisphere damage and may therefore associate with distinct whole-brain and contralateral gradients) (Margulies et al., 2016). Finally, recent work utilizing dense sampling in typical adults (Gordon et al., 2017) and the development of connectome fingerprinting would allow us to explore, at the level of a single-subject, the relationship of contralateral FC with behavior, as well as to examine the inter- and intrasubject variability in contralateral FC [and, wherever possible, systematic variability may explain behavior (Gratton et al., 2018)].

We also acknowledge limitations to this study. We used mass univariate modeling to explore the impact of lesion within the contralateral hemisphere's FC, and having controlled for these multiple comparisons, may have increased type II error. However, there are benefits to this type of modeling, in that connections that reach significance—hundreds that we have shown here—are likewise important and unlikely to be false positive (type I error). These connections can drive *a priori* hypotheses for the future work we have discussed. While not a limitation, another caveat to this study is that the population of study was those with residual (chronic) functional impairments poststroke, thus reflecting a sample that invariably had larger, and more impactful, lesions. Other works investigating contralateral functional brain reorganization poststroke have been earlier in the reorganization time line (i.e., subacute) and also those whose functional impairments were likely to resolve within the spontaneous recovery window (Siegel et al., 2016, 2018). Therefore, the results we provide here are specific to those with residual impairment many months after stroke, and should be interpreted as such.

Conclusion

Several studies reported a poststroke increase of brain activity in the contralateral hemisphere [see reviews by Grefkes and Fink (2014), and by Cocquyt and associates (2017)]. Our study describes an important complementary result: chronic poststroke damage is associated with increased FC within the contralateral hemisphere. This association is more evident in several long-range connections, some of which involve contralateral hubs. Moreover, certain regions are more likely to have an impact on contralateral FC when damaged. Overall, we believe that the association between patterns of damage and patterns of increased contralateral FC opens a promising new direction in studying brain networks and their response to stroke.

Authors' Contributions

G.Y.: conceptualization of work; acquisition, analysis, and interpretation of data; writing of article. B.C.S.: acquisition, analysis, and interpretation of data; writing and revision of article. J.F.: conceptualization of work; acquisition, analysis, and interpretation of data; revision of article. L.B.: acquisition and interpretation of data; revision of article. C.R.: acquisition, analysis, and interpretation of data; revision of article.

Author Disclosure Statement

No competing financial interests exist.

Funding Information

This work was supported by the National Institute on Deafness and Other Communication Disorders (Grant Nos. DC008355 and DC009571 to J.F., C.R., and L.B.).

Supplementary Material

Supplementary Figure S1
Supplementary Figure S2

References

Adhikari MH, Hacker CD, Siegel JS, et al. 2017. Decreased integration and information capacity in stroke measured by whole brain models of resting state activity. Brain 140:1068–1085.

Allen EA, Damaraju E, Plis SM, et al. 2014. Tracking whole-brain connectivity dynamics in the resting state. Cereb Cortex 24:663–676.

Anglade C, Thiel A, Ansaldo AI. 2014. The complementary role of the cerebral hemispheres in recovery from aphasia after stroke: a critical review of literature. Brain Inj 28:138–145.

Ashburner J, Friston KJ. 2005. Unified segmentation. Neuroimage 26:839–851.

Baldassarre A, Ramsey L, Hacker CL, et al. 2014. Large-scale changes in network interactions as a physiological signature of spatial neglect. Brain 137:3267–3283.

Bannister LC, Crewther SG, Gavrilescu M, et al. 2015. Improvement in touch sensation after stroke is associated with resting functional connectivity changes. Front Neurol 6:165.

Benjamini Y, Hochberg Y. 1995. Controlling the false discovery rate: a practical and powerful approach to multiple testing. J R Stat Soc Series B Methodol 57:289–300.

Betzel RF, Medaglia JD, Bassett DS. 2018. Diversity of mesoscale architecture in human and non-human connectomes. Nat Commun 9:346.

Bonilha L, Nesland T, Rorden C, et al. 2014. Mapping remote subcortical ramifications of injury after ischemic strokes. Behav Neurol 2014:215380.

Carmichael ST, Wei L, Rovainen CM, et al. 2001. New patterns of intracortical projections after focal cortical stroke. Neurobiol Dis 8:910–922.

Carrera E, Tononi G. 2014. Diaschisis: past, present, future. Brain 137:2408–2422.

Carter AR, Astafiev SV, Lang CE, et al. 2010. Resting interhemispheric functional magnetic resonance imaging connectivity predicts performance after stroke. Ann Neurol 67:365–375.

Cocquyt EM, De Ley L, Santens P, et al. 2017. The role of the right hemisphere in the recovery of stroke-related aphasia: a systematic review. J Neurolinguistics 44:68–90.

Cohen J, Cohen P. 1983. Applied Multiple Regression/Correlation Analysis for the Behavioral Sciences, 2nd ed. Hillsdale, NJ: Laurence Erlbaum Associates.

Di Pino G, Pellegrino G, Assenza G, et al. 2014. Modulation of brain plasticity in stroke: a novel model for neurorehabilitation. Nat Rev Neurol 10:597.

Faskowitz J, Esfahlani FZ, Jo Y, et al. 2020. Edge-centric functional network representations of human cerebral cortex reveal overlapping system-level architecture. Nat Neurosci 23:1644–1654.

Finn ES, Shen X, Scheinost D, et al. 2015. Functional connectome fingerprinting: identifying individuals using patterns of brain connectivity. Nat Neurosci 18:1664.

Hartwigsen G, Saur D. 2019. Neuroimaging of stroke recovery from aphasia—Insights into plasticity of the human language network. Neuroimage 190:14–31.

Gili T, Fiori V, De Pasquale G, et al. 2017. Right sensory-motor functional networks subserve action observation therapy in aphasia. Brain Imaging Behav 11:1397–1411.

Golestani AM, Tymchuk S, Demchuk A, et al.; VISION-2 Study Group. 2013. Longitudinal evaluation of resting-state FMRI after acute stroke with hemiparesis. Neurorehabil Neural Repair 27:153–163.

Gordon EM, Laumann TO, Gilmore AW, et al. 2017. Precision functional mapping of individual human brains. Neuron 95: 791–807.e7.

Gratton C, Laumann TO, Nielsen AN, et al. 2018. Functional brain networks are dominated by stable group and individual factors, not cognitive or daily variation. Neuron 98: 439–452.e5.

Grefkes C, Fink GR. 2014. Connectivity-based approaches in stroke and recovery of function. Lancet Neurol 13:206–216.

Joliot M, Jobard G, Naveau M, et al. 2015. AICHA: an atlas of intrinsic connectivity of homotopic areas. J Neurosci Methods 254:46–59.

Kang N, Weingart A, Cauraugh JH. 2018. Transcranial direct current stimulation and suppression of contralateral primary motor cortex post-stroke: a systematic review and meta-analysis. Brain Inj 32:1063–1070.

Kertesz A. 2007. *The Western Aphasia Battery-Revised*. New York, NY: Grune & Stratton.

Lindau NT, Bänninger BJ, Gullo M, et al. 2013. Rewiring of the corticospinal tract in the adult rat after unilateral stroke and anti-Nogo-A therapy. Brain 137:739–756.

Margulies DS, Ghosh SS, Goulas A, et al. 2016. Situating the default-mode network along a principal gradient of macroscale cortical organization. Proc Natl Acad Sci U S A 113: 12574–12579.

Mišić B, Fatima Z, Askren MK, et al. 2014. The functional connectivity landscape of the human brain. PLoS One 9 : e111007.

Nachev P, Coulthard E, Jäger HR, et al. 2008. Enantiomorphic normalization of focally lesioned brains. Neuroimage 39: 1215–1226.

Nair VA, Young BM, La C, et al. 2015. Functional connectivity changes in the language network during stroke recovery. Ann Clin Transl Neurol 2:185–195.

New AB, Robin DA, Parkinson AL, et al. 2015. Altered resting-state network connectivity in stroke patients with and without apraxia of speech. Neuroimage 8:429–439.

Overman JJ, Clarkson AN, Wanner IB, et al. 2012. A role for ephrin-A5 in axonal sprouting, recovery, and activity-dependent plasticity after stroke. Proc Natl Acad Sci 109: E2230–E2239.

Power JD, Barnes KA, Snyder AZ, et al. 2012. Spurious but systematic correlations in functional connectivity MRI networks arise from subject motion. Neuroimage 59:2142–2154.

Rorden C, Bonilha L, Fridriksson J, et al. 2012. Age-specific CT and MRI templates for spatial normalization. Neuroimage 61:957–965.

Rubinov M, Sporns O. 2010. Complex network measures of brain connectivity: uses and interpretations. Neuroimage 52: 1059–1069.

Sandberg CW. 2017. Hypoconnectivity of resting-state networks in persons with aphasia compared with healthy age-matched adults. Front Hum Neurosci 11:91.

Saur D, Lange R, Baumgaertner A, et al. 2006. Dynamics of language reorganization after stroke. Brain 129:1371–1384.

Shahid H, Sebastian R, Schnur TT, et al. 2017. Important considerations in lesion-symptom mapping: illustrations from studies of word comprehension. Hum Brain Mapp 38:2990–3000.

Siegel JS, Ramsey LE, Snyder AZ, et al. 2016. Disruptions of network connectivity predict impairment in multiple behavioral domains after stroke. Proc Natl Acad Sci 113:E4367–E4376.

Siegel JS, Seitzman BA, Ramsey LE, et al. 2018. Re-emergence of modular brain networks in stroke recovery. Cortex 101:44–59.

Sporns O, Chialvo DR, Kaiser M, et al. 2004. Organization, development and function of complex brain networks. Trends Cogn Sci 8:418–425.

Tang C, Zhao Z, Chen C, et al. 2016. Decreased functional connectivity of homotopic brain regions in chronic stroke patients: a resting state fMRI study. PLoS One 11:e0152875.

Thomalla G, Glauche V, Weiller C, et al. 2005. Time course of wallerian degeneration after ischaemic stroke revealed by diffusion tensor imaging. J Neurol Neurosurg Psychiatry 76: 266–268.

van den Heuvel MP, Sporns O. 2013. Network hubs in the human brain. Trends Cogn Sci 17:683–696.

Wahl AS, Omlor W, Rubio JC, et al. 2014. Asynchronous therapy restores motor control by rewiring of the rat corticospinal tract after stroke. Science 344:1250–1255.

Xu H, Qin W, Chen H, et al. 2014. Contribution of the resting-state functional connectivity of the contralateral primary sensorimotor cortex to motor recovery after subcortical stroke. PLoS One 9:e84729.

Yang M, Li J, Li Z, et al. 2017. Whole-brain functional connectome-based multivariate classification of post-stroke aphasia. Neurocomputing 269:199–205.

Zhang Y, Wang L, Yang J, et al. 2017. Abnormal functional networks in resting-state of the sub-cortical chronic stroke patients with hemiplegia. Brain Res 1663:51–58.

Address correspondence to:
Brielle C. Stark
Department of Speech, Language and Hearing Sciences
Indiana University
Bloomington, IN 47405
USA

E-mail: bcstark@iu.edu